

Experimental and Numerical Investigations of Forced Convection in Tube-Type Heat Exchanger

Christian Okechukwu Osueke, Igbinosalkpotokin,

Department of Mechanical Engineering, Landmark University, Omu-Aran, Kwara State Nigeria

Abstract:- Experimental and numerical studies of forced convection heat transfer in tube-type heat exchanger consisting four columns of five cylindrical tubes arranged so that every second column is displaced (i.e. staggered configuration) were carried out. Experiments were conducted to determine the effects of flow pattern on heat transfer and pressure drop within the heat exchanger and the heat transfer dependence on position. In the analytical approach, the dimensionless representations of the rates of forced convection (i.e. Nusselt number) and pressure loss (i.e. drag coefficient) were obtained. The numerical simulation is carried out using **FEMLAB 3.0** and the results compared favourably with the experimental. The flow visualization features such as boundary layer developments between tubes, formation of vortices, local variations of the velocity and temperature distribution within the heat transfer device were revealed by numerical solution. The results showed that the average Nusselt number increases with increasing Reynolds number and the heated element position in the bank. The drag coefficient decrease with increasing Reynolds numbers.

Keywords:- Tube-type heat exchangers, staggered tube bank, forced convection.

I. INTRODUCTION

The process of forced convection heat transfer to or from tube bank was the subject of many theoretical and experimental studies because of their relevance in many engineering applications. This process is significant in the design of heat transfer process devices such as boiler for steam generation and cooling coil of air conditioning system.

The increasing interest in developing compact, and high efficient heat exchanger motivated researchers to study heat transfer from tube bank of circular cross section (Keys and London, 1998).

The studied tube-type heat exchanger is a staggered arrangement of four columns of five parallel cylinders. The configuration is determined by tube diameter and longitudinal and transverse pitches which are distances between tube centres. In this heat transfer device, fluid flow perpendicular to the tube bank thus simulating a typical cross flow heat exchanger, used in many industrial applications such as boilers, automotive, air conditioner, etc.

The fluid flow conditions within the bank are dominated by turbulence because most heat exchangers operate at high Reynolds numbers (Re) and induced vortex shedding which enhanced the heat transfer process. The turbulence intensity and its generation are governed by the bank geometry and Re . It was observed that with shorter transverse pitches, the velocity fluctuations become more intensive. The turbulence level of the main flow can influence fluid flow only over the first and second rows (Mehrabian, 2007). A tube bank acts as a turbulent grid and establishes a particular level of turbulence. The heat transfer conditions stabilize, such that little change occurs in the convection coefficient for tube beyond the fifth row tube (Yoo et al, 2007).

For optimal design of heat transfer process device and the determination of its operational performance parameters, the drag, and heat transfer associated with fluid flow over the tube surfaces have to be known. Because a sudden changes in these quantities can lead to hysteresis and poor device functionality (Yukio et al, 2010).

Although reasonable number of researchers had conducted experiments and numerical analyses on fluid flow and heat transfer at the tube bank, but different correlation equations have been proposed to predict the heat transfer or the Nusselt number. The results obtained depend on the geometric configuration, number of tube rows, and the Reynolds number. For example, (Zukauskas, 1987) obtained a correlation given as

$$Nu = C Re^m Pr^n \left(\frac{Pr}{Pr_w} \right)^{0.25} \quad 1$$

where Pr_w and Pr represent the Prandtl numbers evaluated at the wall temperature and the bulk mean temperature, respectively. Re denotes the Reynolds number evaluated at the bulk mean temperature, and it is based on the average velocity through the least cross section formed by the tube array. The constants C , m , and n vary depending on the Reynolds number and tube bundle geometry and it can be found in many heat transfer textbooks.

Generally, a correction factor is always introduced in heat transfer coefficient correlation for number of tube rows because the shorter the bank, the lower the average heat transfer. The influence of the number of tube rows becomes negligible only for $N > 16$ (Incropera and Dewitt 2004).

The pressure drop in tube-type heat exchanger is related to the drag coefficient according to the following equation (Kays & London, 1998).

$$\Delta P = \xi N_R \frac{1}{2} \rho V^2 \quad 2$$

The focus of this study is to conduct experimental and numerical investigations to determine the heat transfer coefficient between a heated cylindrical copper element and the air flow characteristics as it passes through a tube-type heat exchanger. The experimental data was then correlated by power-law curve fitting to obtain the Nusselt number. Furthermore, the experimental data was also used to compute the pressure loss coefficient which represents the pressure drop imposed on the flow by each successive row of tubes. The numerical technique allows flow visualization and temperature distribution within the heat exchanger.

II. MATERIALS AND METHODS

Experimental Technique

The experimental technique is essential to produce cooling curves of heated element for different flow conditions. The primary component of the tube-type heat exchanger (i.e. test apparatus) is valve controlled air flow duct with a perspex test section of 125mm x 125mm through which air is drawn by a centrifugal fan, and into which the heated element under investigation is inserted as shown in Fig 1.

Air temperature upstream of the test section and atmospheric pressure were obtained by means of thermocouple and mercury barometer respectively.

Air pressure differential upstream and downstream of the test section were measured by inclined water manometer connected to the head tube located in the centre upstream position with the tube itself on the horizontal centerline of the test section, and it faced upstream as shown in Fig 1. The velocity upstream the test section is established from the pressure drop between atmosphere and upstream static pressure tapping (i.e. depression of water column the manometer) and is recorded H_1 in meters. The sampled result is as shown in Table 3.

Heat transfer measurements were obtained by replacing one of the Perspex rods with an externally identical heated copper rod. The copper rod outer and inner diameter are 12.45mm and 11.5mm respectively and its length is 95mm. It is carried between two extension rods of fabricated plastic compound. The element temperature is obtained by K-type 0.2 mm diameter thermocouple probe inserted at its centre. The thermocouple output is connected to a digital multimeter (MAS-34X model) which also was connected to a Pentium 3 desktop computer as shown in Fig 1.

The test procedure involved heating the copper rod with electrical heater to 70°C above air flow temperature outside the test section. Thereafter, it is inserted at different desired positions in the test section (i.e. centre of 1st, 2nd, 3rd and 4th columns) under different flow conditions such as 10, 20, 30, 40, 50, 60, 70, 80, 90 and 100% throttle openings. Then its temperature and time of cooling were recorded with the thermocouple embedded at its centre. The heat transfer coefficient is then deduced from logarithm plot (Fig 3.0) of rate of cooling together with the knowledge of the thermal capacity and surface area of the copper.

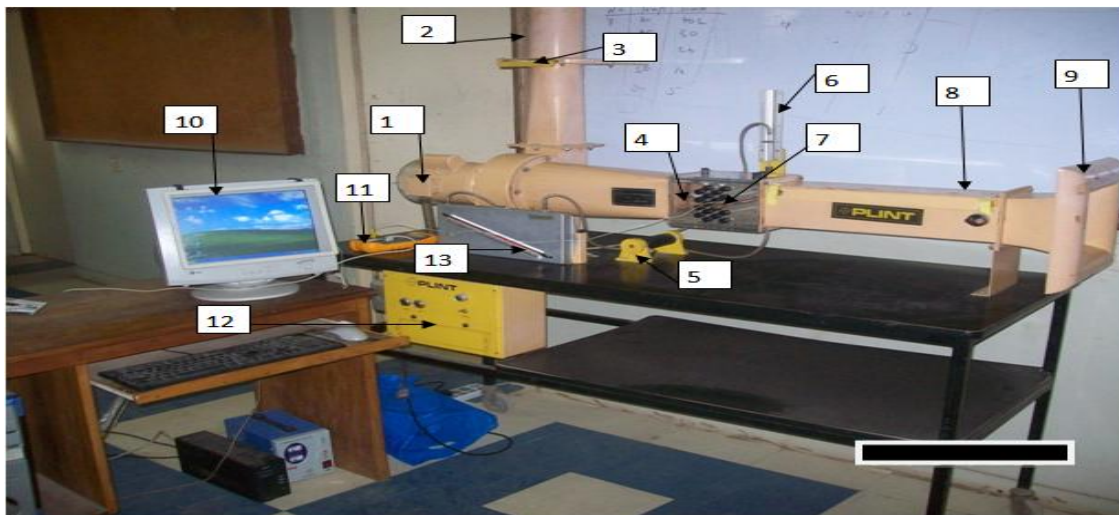


Fig.1: Cross flow tube-type heat exchanger experimental test rig.

Where

1. Fan, 2. Air discharge tube, 3. Throttle valve, 4. Working section, 5. Electric heater, 6. Total head tube, 7. Test element, 8. Thermometer, 9. Bellmouth, 10. Computer, 11. Digital multimeter, 12. Control panel and 13. Inclined manometer.

Basic assumptions and problem formulation

It was assumed that the heat generated in the cylindrical copper element is transferred to the air that flowing through it. However, a certain amount of heat is conducted from the element into the plastic extension pieces. A correction factor of 8.4mm was used to compensate for plastic extension (Plint and Partners Ltd, 1981). Therefore:

$$L_1 = L + 0.0084 \quad 3$$

It was further assumed that temperature gradients within the element are negligible, so that the thermocouple embedded at the centre gives a true reading of the effective surface temperature. The justification for this assumption is that the Biot number is very small ($Bi < 0.1$).

The rate of heat transfer from the element to the air stream is given by:

$$q = hA(T - T_a) \quad 4$$

The temperature drop dT in a period of time dt is given by:

$$-qdt = mcdT \quad 5$$

Combining Equations (4) and (5) gives:

$$\frac{-dT}{(T - T_a)} = \frac{hA_1}{mc} dt \quad 6$$

where A is replaced by A_1 to allow for the tube plastic extensions. Integrating equation (6), we obtain:

$$\log_e(T - T_a) - \log_e(T_o - T_a) = \frac{-hA_1 t}{mc} \quad 7$$

Equation (7) suggests that a plot of $\log_e(T - T_a)$ against t yield a straight line slope

$$M = \frac{-hA_1}{mc} \quad 8$$

and since we can obtained the other factors in this expression from the geometrical properties of copper in table 1., the heat transfer coefficient is related to the slope M of this line by the following expression:

$$h = \frac{-mc}{A_1} M \quad 8$$

A plot of $\log_{10}(T - T_a)$ against time (t) was used, since $\log_e N = 2.3026 \log_{10} N$.

The effective velocity of the air across the element is determined by calculating the velocity V_1 upstream. The velocity V_1 developed by gas of density ℓ expanding freely from rest under the influence of pressure difference P . When P is sufficiently small for compressibility to be neglected, then, applying Bernoulli's equation gives:

$$\frac{\ell V_1^2}{2} = P \quad 9a$$

the pressure head H_1 was measured in centimeters of water. Since

$$1 \text{ cm } H_2O = 98.1 \text{ N/m}^2$$

equation (9a) becomes

$$\frac{\ell V_1^2}{2} = 98.1 H_1 \quad 9b$$

The density of air under pressure P_a and at temperature T_a is given by ideal gas equation.

$$P_a = RT_a \quad 10$$

where the gas constant $R = 2875 \text{ J/kmol.K}$

substituting equation (9) in (10) yields:

$$V_1 = 237.3 \sqrt{\frac{H_1 T_a}{P_a}} \quad 11$$

Equation (11) is used for calculating local velocities upstream of the test section.

The calculation of the effective velocity through bank of tubes was based on the minimum flow area. When all the tubes are in position, the minimum area occurs in a transverse plane. Therefore,

$$V = 2V_1 \quad 12$$

Dimensional analysis shows that the relationship between h and the independent variables is expressed as:

$$\frac{hD}{K} = Nu \quad 13$$

$$Re = \frac{\rho V D}{\mu} \quad 14$$

$$Pr = \frac{C_p \mu}{K} \quad 15$$

The pressure drop is expressed as a proportion to the velocity head. It represents the pressure drop imposed on the flow by each successive rank of tubes which is represented as:

$$H_3 = H_1 - H_2 \quad 16$$

and the drag coefficient is calculated as:

$$C_D = \frac{H_3}{4H_1} \quad 17$$

III. NUMERICAL MODELLING

Numerical simulation technique was essential for flow visualization and temperature distribution within the heat exchanger. The simulation modeling was performed in a two-dimensional domain, which represents the test section as shown in Fig2. FEMLAB 3.0 software was used to draw all parts in computational domain and to generate grids. The dimensions of computational domain were idealized to reveal the fundamental issues and enable validation with the experimental data that was the reason why this computational domain only cover the test section. This computational domain has a length and width as same size with the experimental test section.

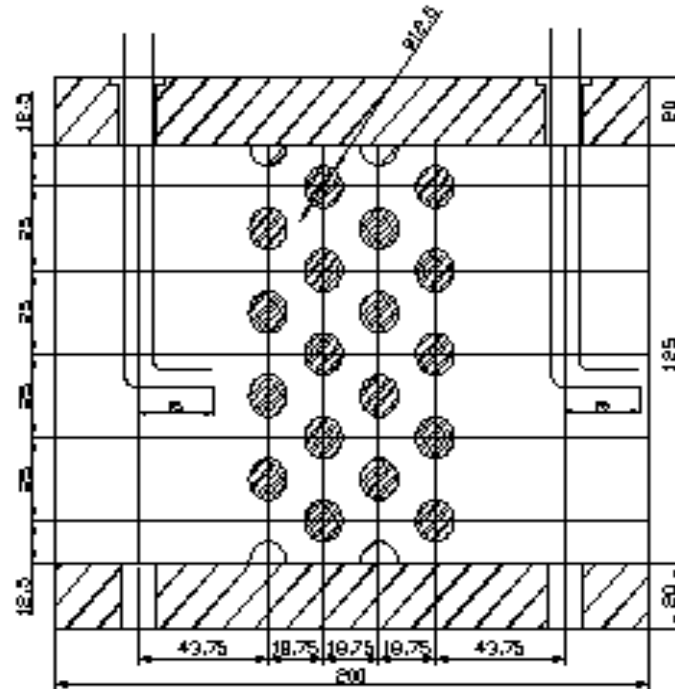


Fig.2: Schematic diagram of a staggered tube bank working section.

Since the governing equations are in spatial coordinates, the boundary conditions were provided for all boundaries of the computation domain. At the up-stream boundary, uniform flow velocity U_{in} and temperature T_{in} were assumed. At the down-stream end of the computational domain, the Neumann boundary condition was applied. At the solid cylinder surfaces represented by circles, no-slip conditions and thermal insulation were applied, while constant temperature T_{tube} was specified for the heated element. At the symmetry plane, normal velocity and the temperature variation along the normal direction were set to zero.

IV. RESULTS AND DISCUSSION

Experimental and numerical simulations of heat transfer and fluid flow characteristics of tube-type heat exchanger with staggered configuration are presented.

For these studies, the following dimension and fluid properties used are presented in tables 1 and 2 respectively.

Table 1. Geometrical properties of the copper rod.

Description	Quantity	Unit
External diameter (d)	12.45	mm
Internal diameter (d _i)	11.5	mm
Thickness of tube (t)	0.5	mm
Length of tube (l)	95	Mm
Effective length (l ₁)	0.1304	M
Surface area (A)	0.00371	m ²
Effective surface area (A ₁)	0.00404	m ²
Specific heat (C)	380	J/kg.K
Mass (m)	0.0274	Kg

Table 2. Properties of the fluid (air).

Description	Quantity	Unit
Ambient temperature (T _a)	300	°K
Barometric pressure (P _a)	99,042	N/m ²
Density of air at T _a (ρ)	1.1614	kg/m ³
Dynamic viscosity (μ)	1.846X10 ⁻⁵	kg/ms
Thermal conductivity (K)	0.0263	J/msoC

In a particular test, the heated element was inserted at the centre position in the first column of tubes with the apparatus running, the results obtained for different set flow rate are in the ranges of 10 – 100% and are presented in table 3. The rate of cooling resulting from minimum flow rate of 10% is shown in Fig 3. The pressure differential H₃ imposed on the flow by each successive column of tube across the exchanger was obtained with all the tubes in position and the test result is shown in Fig 4.

Table 3.0: Data Corresponding to Ten Different Throttle Openings when the Heated Element is positioned at the centre of 1st column.

Throttle opening (%)	H ₁ (cmH ₂ O)	V ₁ (m/s)	V (m/s)	Re	M (s ⁻¹)	H (J/ms ² C)	Nu
10	0.03	2.263	4.524	3543	-0.009	53.4182	25.28732
20	0.18	5.541	11.082	8680	-0.011	65.28891	30.90673
30	0.33	7.502	15.005	11753	-0.011	65.28891	30.90673
40	0.48	9.048	18.097	14175	-0.012	71.22427	33.71643
50	0.64	10.448	20.896	16367	-0.013	77.15962	36.52613
60	0.79	11.608	23.216	18187	-0.013	77.15962	36.52613
70	0.94	12.662	25.325	19836	-0.013	77.15962	36.52613
80	1.096	13.673	27.345	21418	-0.013	77.15962	36.52613
90	1.248	14.59	29.18	22856	-0.013	77.15962	36.52613
100	1.42	15.563	31.126	24380	-0.014	83.09498	39.33583

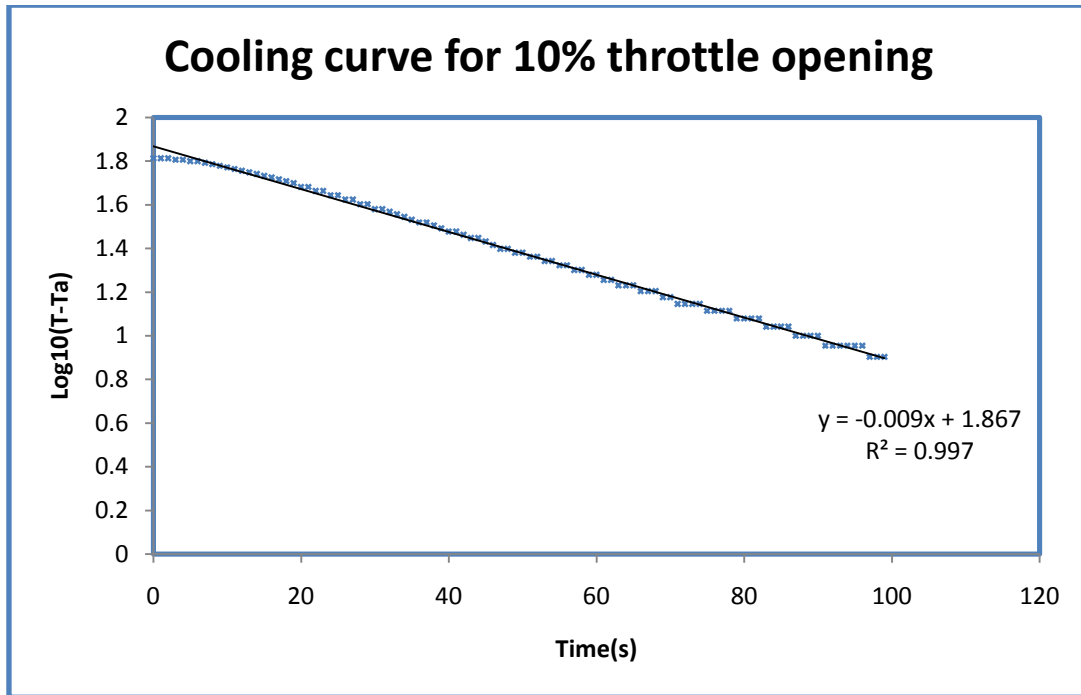


Fig. 3: A plot of $\log_{10}(T-T_a)$ against t for 10% throttle opening.

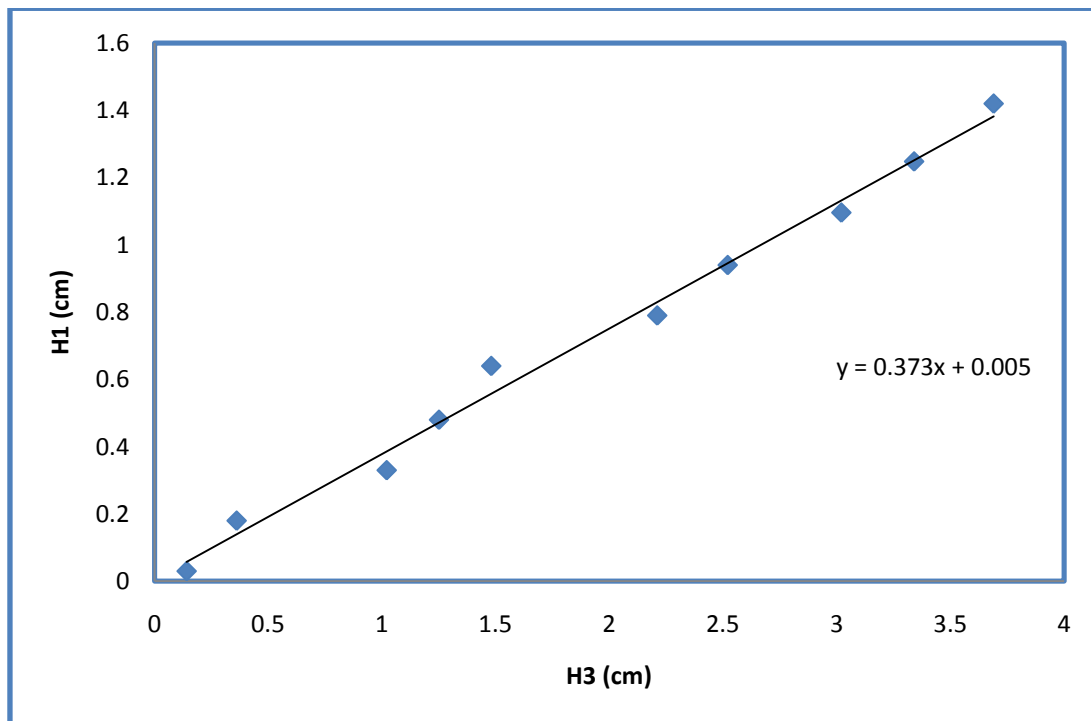


Fig. 4: Pressure differential across the tube bank.

Dimensionless quantities such as Reynolds number, drag coefficient and Nusselt number were calculated using the relevant equations. The drag coefficient which represents the pressure drop was calculated using equation (17) and the results were plotted against Reynolds number is shown in Fig.5. In the case of Reynolds number equation (14) was used, while equation (13) was used to calculate the Nusselt number. The results are shown in table 3. Furthermore, empirical correlation for heat transfer coefficient was obtained with power-law curve fitting. The curves are shown in Fig. 6 and the resulting correlation are shown in table 4.

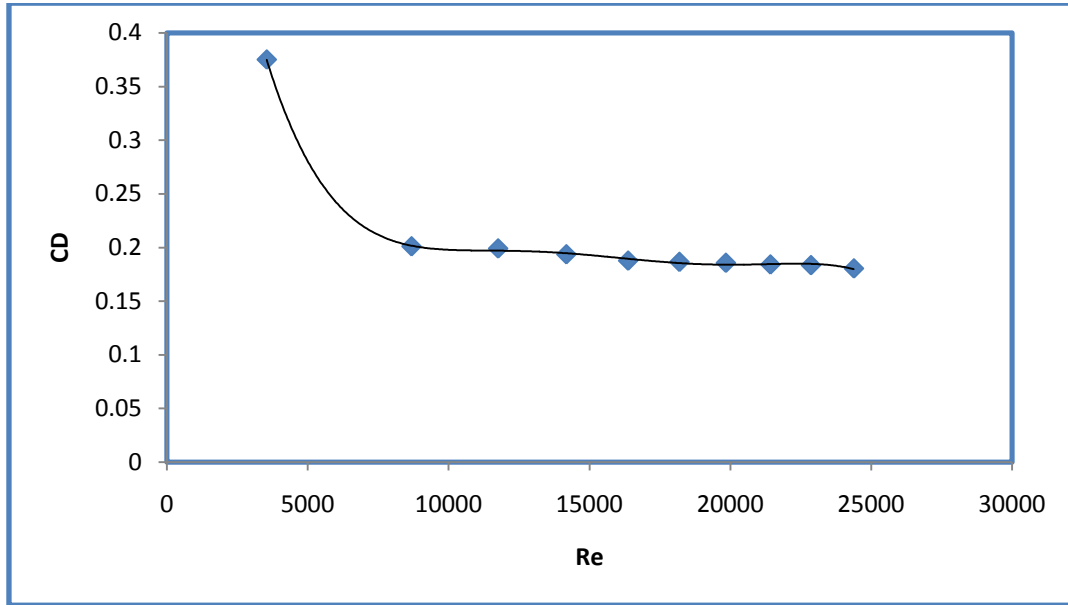


Fig. 5: Drag coefficient vs. Reynolds number.

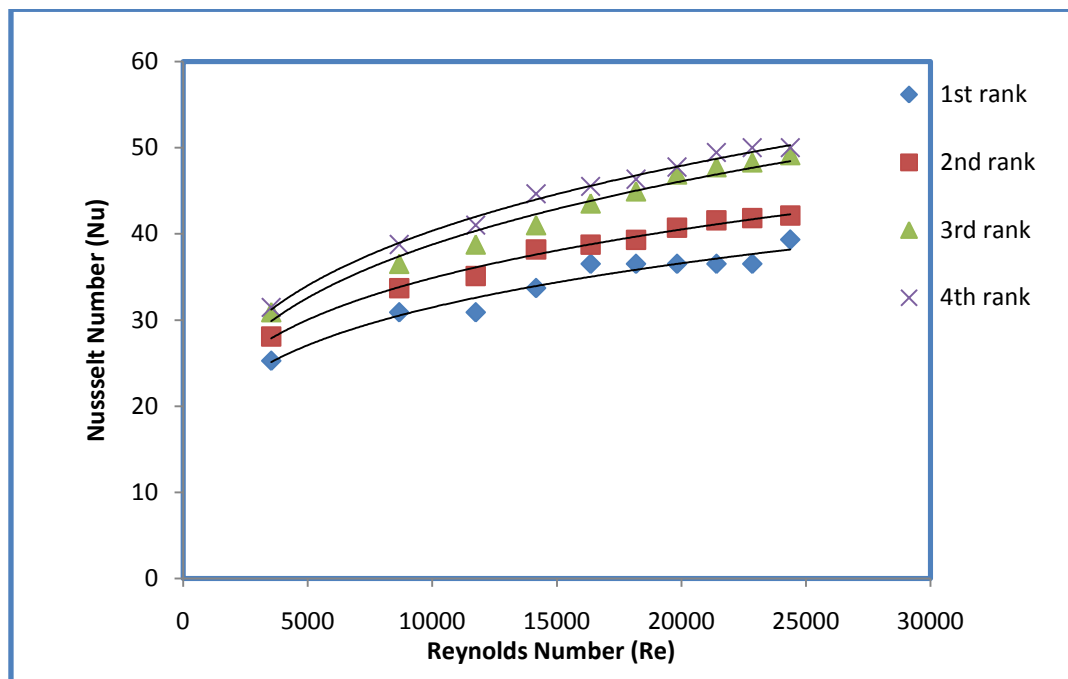


Fig. 6: Relationship between experimental Nu and Re for cross flow of air that past the tube bank

Table 4: Experimental results showing Nu and Re relationship.

Rows	Experimental Correlations
1 st	$Nu = 4.125Re^{0.24}$ $R^2 = 0.952$
2 nd	$Nu = 3.858Re^{0.25}$ $R^2 = 0.990$
3 rd	$Nu = 4.758Re^{0.216}$ $R^2 = 0.972$
4 th	$Nu = 4.258Re^{0.271}$ $R^2 = 0.993$

Numerical results
Velocity Distribution

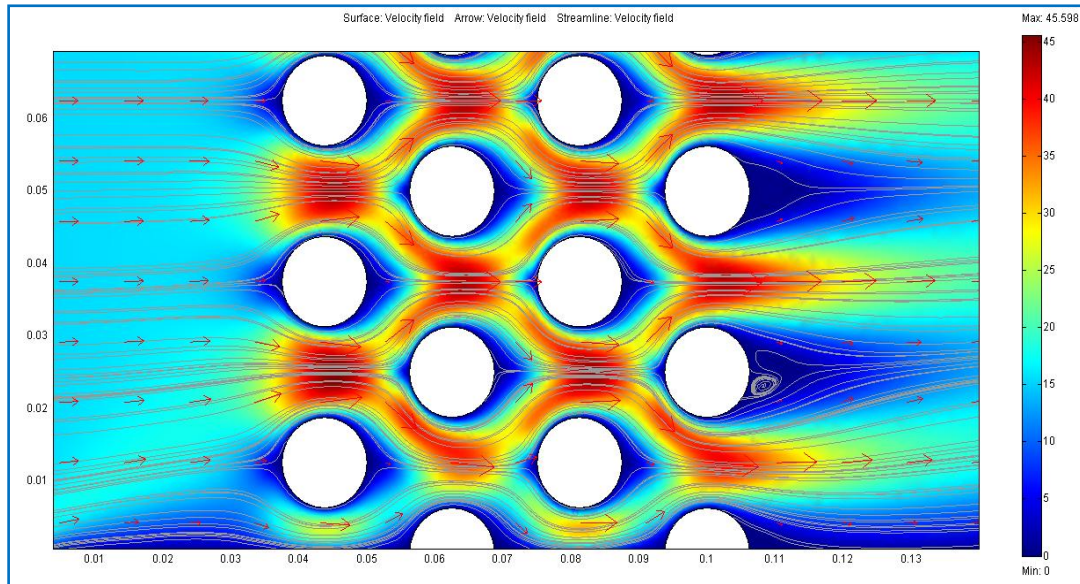


Fig. 7: Velocity distribution in the tube bank at $Re = 24380$

Velocity pattern in the bank is illustrated in Fig.7. Fluid velocity in the mid-plane of the tubes was observed to be higher and weak near tube surface plane because of the boundary layer development on the surface. A detailed inspection of the Figure shows that higher percentage of fluid stream is imposed upon the heated tube surface. As a result of this, relatively smaller wake region was developed. It can also be seen that the main flow that passed through every tube rank and the flow are well mixed. This in turn enhances the heat transfer. The streamline plot revealed that vortex formation occurs in the zones of recirculation. However, the region was much larger behind the last column of cylinders for low Reynolds number.

Boundary Layer Separation

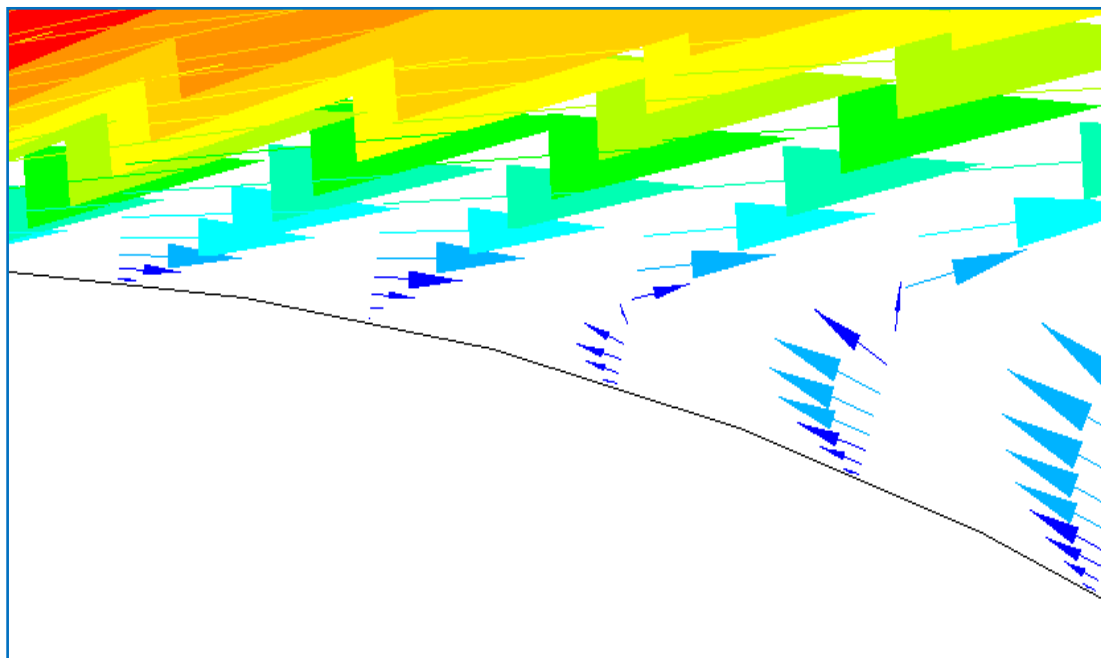


Fig. 8: The boundary layer separation point of first rank in tube bank at $Re = 24380$

Boundary layer separation occurs at a point on the tubes where the fluid momentum is too weak to overcome the adverse pressure gradient and then detached from the tubes surface as shown in figure 8.0. This separation was observed shortly after ($\theta = 90^\circ$). By the nature of these flow separations, local heat transfer and fluid mixing increase especially upstream of the tubes and cause low performance at the wake region located downstream of the tubes.

Temperature Distribution

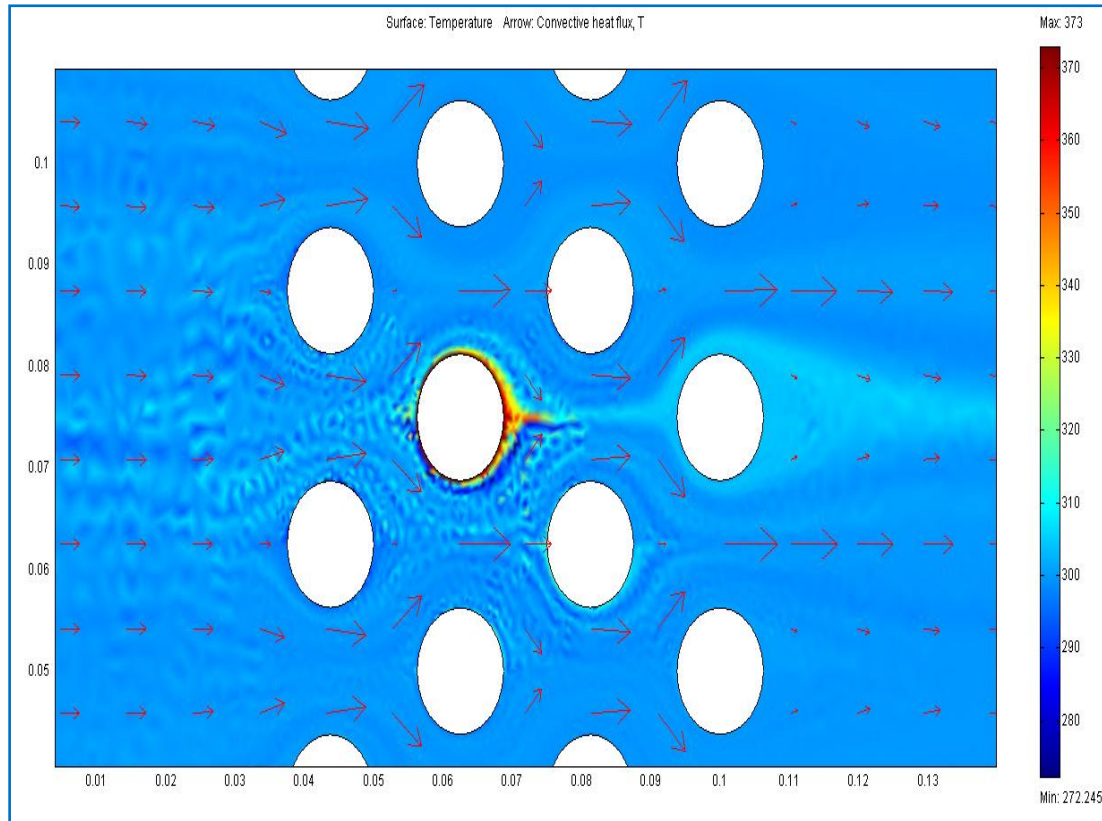


Fig. 9: Temperature distributions in the tube bank at $Re = 24380$.

Figure 9 above shows the temperature distributions within the bank. The cooling rate of the heated element is greater within the tube-mid planes where maximum local velocity occurs. This was evident by the low temperature close to that of the free stream recorded. The temperature gradient near the upstream tube was higher due to the thin boundary layer thickened, while the temperature gradient downstream along the tube is lower than the upstream due to the wake flow.

The numerical data were essentially used to reveal temperature distribution and flow visualizations such as velocity distribution, boundary layer separation occurring within the tube bank. The experimental test was used to generate cooling curves. A logarithm plot for the rate of cooling was produced as shown in Fig. 3. The slope obtained from Fig. 3.0, together with the knowledge of the copper thermal capacity, mass, and surface area were used to calculate heat transfer coefficient between the heated copper element, and the air flow normal to it.

Pressure drop across the tube-type heat exchanger increases with increasing Reynolds. Numerical results were 12% higher than the experimental.

It is observed that the heat transfer coefficient increases, though at a diminishing rate, in successive columns of tubes. This is caused by the increasing level of turbulence and stability as the air passes through the tube bank.

Numerical Nusselt number was 15% higher than that of the experimental results. The discrepancy in result could be due to poor convergence resulting from inability of the software to handle high turbulent flow that was obtained in the experimental work. Both the experimental and numerical predictions indicate that the Nusselt number and pressure drop increase with the increasing Reynolds number.

V. CONCLUSION

The heat transfer coefficient was a function of the heated element position and Reynolds number in the tube bank. Numerical and experimental results compared favourably. The present numerical and experimental investigations suggest that changes in heat transfer from copper tube were dependent on the position and flow pattern (Reynolds number) in the heat exchanger while the pressure drop was a function of the Reynolds numbers. Downstream from the third column, the heat transfer stabilizes, such that little change occurs in the convection coefficient from tube beyond the fourth.

REFERENCES

- [1]. Kays, W. S., London, A. L., 1998, Compact Heat Exchangers, 3rd Ed., KriegerPublishing Company, Malabar, Florida.
- [2]. M. A. Mehrabian, 2007, Heat Transfer And Pressure Drop Characteristics Of Cross Flow Of Air Over An Circular Tube in Isolation And/Or in a Tube Bank, The Arabian Journal for Science and Engineering, Volume 32.
- [3]. S.Y. Yoo, H.K. Kwon, J.H. Kim, 2007, A study on heat transfer characteristics for staggered tube banks in cross-flow, J. Mech. Sci. Technol. Vol. 21 pp505–512.
- [4]. Yukio Takemoto, KeijiKawanishi, JiroMizushima, 2010, Heat transfer in the flow through a bundle of tubes and transitions of the flow, International Journal of Heat and Mass Transfer, Vol. 53 pp 5411–5419
- [5]. Žukauskas, A.,1987, Convective Heat Transfer in Cross Flow, Handbook of Single-Phase
- [6]. Convective Heat Transfer, Wiley & Sons, New York.
- [7]. Incropera F.P. and Dewitt D.P.(2004),Fundamental of Heat and Mass Transfer, 5th ed., John Wiley & Sons, Inc.